



# Reaction mechanism and kinetics for the oxidation of dimethyl sulfide by nitrate radical

Justin Jee, Fu Ming Tao \*

*Department of Chemistry and Biochemistry, California State University, 800 North State College Blvd., Fullerton, CA 92834, USA*

Received 12 October 2005; in final form 30 December 2005

## Abstract

The reaction between dimethyl sulfide ( $\text{CH}_3\text{SCH}_3$ ) and nitrate radical ( $\text{NO}_3$ ) is studied using density functional theory and ab initio methods. The transition state for this reaction is optimized at different levels of theory and basis sets, and then used for kinetics calculations of the rate constant. The  $\text{CH}_3\text{SCH}_3 + \text{NO}_3$  reaction leading to  $\text{CH}_3\text{SCH}_2$  and  $\text{HNO}_3$  is shown to have a negative activation energy and thus negative temperature dependence. The study confirms that the  $\text{NO}_3$  radical is a significant contributor to the oxidation of DMS in the troposphere.

© 2006 Published by Elsevier B.V.

## 1. Introduction

Dimethyl sulfide (DMS) is the most common reduced sulfur compound released by biogenic sources [1]. Released primarily by marine plankton as they metabolize dimethyl sulfoniopropionate (DMSP), this volatile compound establishes a relatively high mixing ratio of 110 ppt above the marine boundary layer [2]. Although DMS quickly reacts with the OH radical during the daytime, its reaction with the nitrate radical ( $\text{NO}_3$ ) is more predominant at night and in areas where nitrate concentration is relatively high [3]. Experiments have been performed on the  $\text{NO}_3 + \text{DMS}$  reaction and  $\text{SO}_2$ , methane sulfonic acid (MSA), and  $\text{CH}_2\text{O}$  have been found among the products. Thus, it is believed that the reaction proceeds via hydrogen abstraction leading immediately to nitric acid and the  $\text{CH}_2\text{SCH}_3$  radical [4]. Tyndall et al. [5] recommends a rate constant of  $1.0 \times 10^{-12} \text{ cm}^3 \text{ molecule}^{-1} \text{ s}^{-1}$  for the reaction based on results of several experiments. However, there has been discrepancy as to the temperature dependence of this reaction. Furthermore, questions have arisen regarding the

possible formation of an adduct preceding the hydrogen abstraction reaction [4].

In this study, ab initio and density functional theory (DFT) calculations are performed on the  $\text{DMS} + \text{NO}_3$  reaction along stationary points. The calculated energies, geometries, and frequencies provide details about the reaction pathway and kinetics of the  $\text{DMS} + \text{NO}_3$  reaction that are used to clarify results from experiments.

## 2. Methods

### 2.1. Quantum chemical methods

This study used four different DFT functionals: Becke's 3-parameter functional with corrections by Lee, Yang, and Parr (B3LYP); Becke's half and half functional with the same corrections (BH&HLYP); the metahybrid exchange-correlation functional, BB1K; and the metahybrid density functional theory, MPWB1K. B3LYP has been known to systematically underestimate reaction barrier heights, particularly for hydrogen abstraction, and is only included for comparison to other theories. BH&HLYP has been known to provide barrier heights more consistent with experiments [6]. BB1K and MPWB1K are two metahybrid density functional methods that have recently been shown

\* Corresponding author. Fax: +1 714 278 5316.

E-mail address: [ftao@fullerton.edu](mailto:ftao@fullerton.edu) (F.M. Tao).

to produce results for accurate kinetics calculations [7]. Results from the DFT methods are compared to those of second-order Møller–Plesset perturbation theory, MP2, and coupled cluster theory with single, double, and triple excitations, CCSD(T). Although MP2 generally gives accurate geometries for reaction complexes, it also overestimates barrier heights [6,8]. Thus, CCSD(T) single-point energy calculations were performed on MP2 geometries optimized at the aug-cc-pVDZ basis set, particularly at the transition state. Otherwise, reported data uses Pople's basis sets 6-31+G(d) and 6-311++G(d,p) as implemented in the GAUSSIAN 03 program [9].

## 2.2. Kinetics

Kinetics calculations were performed on optimized reactants, products, and transition states in order to obtain theoretical rate constants at different temperatures. These calculations were carried out using the online services provided by the Truong research group at the University of Utah [11]. The calculations are based on classical transition state theory and utilize frequencies, symmetries, moments of inertia, and activation energy to achieve a projected rate constant. Eckart tunneling corrections were applied to the MP2 predicted reaction due to its high positive energy barrier of 9 kcal/mol. No tunneling corrections were made for other theoretical results on the reaction pathway because of the predicted negative activation energy. Calculated Gibbs free energies of the reaction were used to obtain equilibrium constants.

## 3. Results and discussion

### 3.1. Quantum chemical calculations

The optimized geometries using various theoretical methods and basis sets appeared to converge on a common reaction pathway involving the formation of a reactant complex (RC), transition state, product complex (PC),

and separate products ( $\text{HNO}_3 + \text{CH}_2\text{SCH}_3$ ). Fig. 1 shows the optimized geometries at the MP2/aug-cc-pVDZ level for the reactant complex, transition state, and product complex. B3LYP and BH&HLYP predict a relatively high binding energy of at least 14.3 kcal/mol for the RC, indicating strong interactions between DMS and the  $\text{NO}_3$  radical. The RC structure shows two short intermolecular bonds: one between the sulfur atom of DMS and an oxygen atom of  $\text{NO}_3$ , 2.27 Å, and the other between a hydrogen atom of DMS and a second oxygen atom of  $\text{NO}_3$ , 2.26 Å. MP2 calculations only predict at most 3.46 kcal/mol although the MP2 geometry of the RC is very similar with those of density functional theory. It is thus clear that a fairly stable adduct complex could form from nitrate and DMS, in agreement with experiments by Jensen et al. [4]. A final note concerning the geometry of the reactant complex is that it exhibits fourfold symmetry. When nitrate reacts with DMS, it could pull off any one of four hydrogen atoms that are close to the sulfur atom (see Fig. 1). This symmetry becomes significant later for kinetics calculations as they cause a fourfold increase in the rate constant of the reaction.

As hydrogen abstraction proceeds, the interaction between the S and O sites characterizing the adduct complex disappears, as shown by the increased distance between the two atoms at the transition state, 2.67 Å. On the other hand, the distance between the H of DMS and the second O of  $\text{NO}_3$  decreases to 1.41 Å at the transition state. Meanwhile, the C–H covalent bond of DMS increases from 1.10 Å at the RC to 1.24 Å at the transition state. Such changes continue until the hydrogen atom is completely abstracted, forming the corresponding reaction products. Note, that the optimized geometries from all methods and basis sets give the similar values for the bond distances.

B3LYP, BH&HLYP, MPWB1K, and BB1K methods predict the  $\text{DMS} + \text{NO}_3$  reaction to have negative activation energy (see Table 1), while MP2 predicts positive activation energy. As expected, B3LYP underestimates

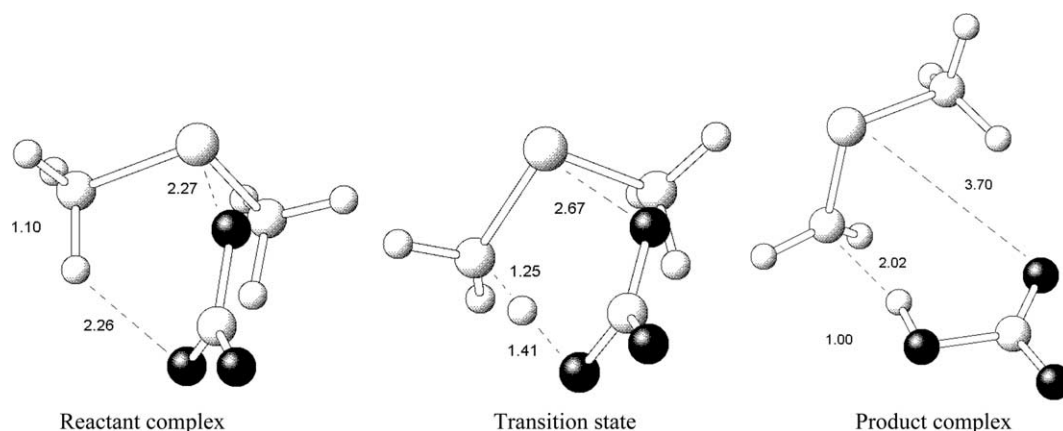


Fig. 1. Geometries of stationary points optimized using MP2/aug-cc-pVDZ corresponding to the reactant complex, transition state, and product complex, respectively. Selected distances are shown in Å.

Table 1

Relative energies, enthalpies, and free energies (in kcal/mol, at 298 K and 1 atm) of the reacting system with respect to separate reactants calculated from various methods and basis sets

Theory/basis set	Electronic energies				ZPE-corrected		Enthalpies		Free energies	
	$\Delta E_{RC}$	$\Delta E^\ddagger$	$\Delta E_{PC}$	$\Delta E$	$\Delta E_{ZP}^\ddagger$	$\Delta E_{ZP}$	$\Delta H^\ddagger$	$\Delta H$	$\Delta G^\ddagger$	$\Delta G$
B3LYP/6-31+G(d)	−14.71	−3.26	−8.80	−1.81	−3.69	−1.07	−4.25	−1.16	5.91	−1.97
B3LYP/6-311++G(d,p)	−14.96	−4.98	−12.40	−5.57	−5.34	−4.72	−5.92	−4.75	4.49	−5.71
MP2/6-31+G(d)	−5.17	10.94	−4.23	4.45	6.77	0.56	6.47	0.89	16.73	−0.62
MP2/6-311++G(d,p)	−1.96	11.24	−6.23	1.36	7.39	−2.35	7.01	−2.00	17.42	−3.50
MP2/aug-cc-pVDZ	−3.65	9.87	−7.23	4.65	5.83	−1.87	5.49	−1.50	15.67	−3.08
BH&HLYP/6-311++G(d,p)	−14.31	−1.80	−17.08	−10.42	−2.85	−10.82	−3.33	−10.59	8.26	−10.95
BB1K/6-311++G(d,p)		−5.05		−10.43	−5.52	−10.16	−6.15	−10.09	5.73	−10.15
MPWB1K/6-311++G(d,p)		−6.02		−10.80	−6.55	−10.65	−7.15	−10.54	4.64	−10.70
CCSD(T)/6-311++G(d,p) <sup>a</sup>		−0.13		−7.68						

<sup>a</sup> Calculated with the MP2/aug-cc-pVDZ geometries.

the energy barrier by about 4 kcal/mol while MP2 predicts an activation energy that is too high. When single-point CCSD(T) calculations are performed on optimized MP2 geometries, the results agree more closely with those of DFT, falling within 2 kcal/mol of BH&HLYP and 4 kcal/mol of B3LYP. Thus, the two most reliable methods, CCSD(T) and BH&HLYP, are in close agreement with each other, indicating that the true activation energy is around −1 kcal/mol. As will be shown, these methods also produce the rate constant most consistent with experiments. When zero-point energy corrections are included in the DFT results, the activation energy drops by about 0.4–1.0 kcal/mol. When zero-point energy corrections are included in the MP2 results, this energy drops even more (by about 4 kcal/mol), further indicating that all levels of theory are converging upon similar activation energy. Finally, this reaction is exothermic according to the results at all levels of theory, and is thermodynamically favorable to form the products. Although the uncorrected relative energy  $\Delta E$  at MP2/aug-cc-pVDZ is positive (4.65 kcal/mol), it drops to −1.87 kcal/mol with zero-point corrections, 0.8 kcal/mol lower than zero-point corrected B3LYP values.

The production of dimethyl sulfoxide (DMSO) + nitrite might be another pathway for the DMS + NO<sub>3</sub> reaction. The B3LYP calculations predict the reaction to have a high energy barrier of at least 10 kcal/mol, suggesting that this pathway is negligible, despite of the result that the reaction is exothermic ( $\Delta E \sim 21$  kcal/mol). Using BH&HLYP and BB1K the activation energy only increases. In fact, no

nitrite is produced from the DMS + NO<sub>3</sub> reaction in experimental studies. As a result, the pathway will not be considered further in this study. This decision is in agreement with experimental studies by Daykin et al. [10].

The present calculations on the hydrogen abstraction reaction do not demonstrate significant dependence on the basis set, especially with regard to geometries and relative electronic energies. The results are also consistent among the different methods except for MP2. The MP2 activation energy is too high, and the reaction energy at the MP2/6-31+G(d) level is positive. The results from CCSD(T) calculations using the MP2 geometries demonstrate that the BH&HLYP method should give the most reliable results. B3LYP, MPWB1K, and BB1K appear to underestimate the activation energy, although the difference among the B3LYP, MPWB1K, and BB1K results is slight (about 1 kcal/mol). The MP2 results and the basis set dependence are also in agreement with other ab initio studies, such as for the DMS reaction with OH radical [6].

### 3.2. Kinetics

Table 2 lists rate constants calculated at different temperatures. These can be compared to Tyndall's suggested value of  $1.0 \times 10^{-12} \text{ cm}^3 \text{ molecule}^{-1} \text{ s}^{-1}$  at 298 K [5]. Clearly BH&HLYP and extrapolated CCSD(T) calculations give the best results, falling within 50% of the empirically accepted value. B3LYP, MPWB1K, and BB1K predict an activation energy that appears too low, and thus rate constants calculated using those theories are one to three orders

Table 2

Rate constants (in  $\text{cm}^3 \text{ molecule}^{-1} \text{ s}^{-1}$ ) obtained from using transition state theory for the CH<sub>3</sub>SCH<sub>3</sub> + NO<sub>3</sub> reaction at different temperatures in K

	260 K	270 K	280 K	290 K	300 K	310 K
B3LYP	$9.960 \times 10^{-11}$	$7.222 \times 10^{-11}$	$5.368 \times 10^{-11}$	$4.080 \times 10^{-11}$	$3.162 \times 10^{-11}$	$2.496 \times 10^{-11}$
MP2 <sup>a</sup>	$7.741 \times 10^{-19}$	$1.077 \times 10^{-18}$	$1.476 \times 10^{-18}$	$1.996 \times 10^{-18}$	$2.666 \times 10^{-18}$	$3.518 \times 10^{-18}$
BH&HLYP	$1.547 \times 10^{-12}$	$1.313 \times 10^{-12}$	$1.131 \times 10^{-12}$	$9.867 \times 10^{-13}$	$8.710 \times 10^{-13}$	$7.769 \times 10^{-13}$
BB1K	$8.318 \times 10^{-10}$	$5.594 \times 10^{-10}$	$3.881 \times 10^{-10}$	$2.768 \times 10^{-10}$	$2.025 \times 10^{-10}$	$1.515 \times 10^{-10}$
MPWB1K	$5.357 \times 10^{-9}$	$3.362 \times 10^{-9}$	$2.188 \times 10^{-9}$	$1.470 \times 10^{-9}$	$1.017 \times 10^{-9}$	$7.226 \times 10^{-10}$
CCSD(T)	$6.902 \times 10^{-12}$	$5.366 \times 10^{-12}$	$4.263 \times 10^{-12}$	$3.453 \times 10^{-12}$	$2.845 \times 10^{-12}$	$2.381 \times 10^{-12}$

<sup>a</sup> Because MP2 theory produced a significant energy barrier Eckhart tunneling was applied to the rate constant calculations.

of magnitude larger than the experimental value. MP2 calculations predict a rate constant that is several orders of magnitude too slow, consistent with the predicted activation energy that is clearly too high.

The result that this reaction exhibits negative activation energy also presents problems concerning the validity of classical transition state theory. Tunneling factors applied to the potential energy surface are nonsensical, and caution must be observed to ensure that the potential is not actually flat as the hydrogen atom is transferred from reactant to product. For these reasons, Eckart tunneling was not applied to calculations with negative activation energy, and the question of whether or not we obtained a ‘true’ transition state was answered by the fact that only one imaginary frequency was obtained at each optimized transition state. The negative activation energy also implies that this reaction clearly exhibits slight negative temperature dependence. This has important atmospheric implications in that it validates the nighttime occurrence of nitrate’s reaction with DMS. Also, because experiments by Daykin et al. [10] refute the possibility of rate dependence on pressure or other external factors it becomes clear that temperature is a major determinant of the rate of DMS oxidation by nitrate. Furthermore, the temperature dependence predicted in this study validates Tyndall’s claim that oxidation of sulfur species by nitrate in general exhibit negative temperature dependence [5]. Finally, it is useful to note that aside from rate constants produced from MP2, the reverse rate constant is at least six orders of magnitude slower than the forward rate constant and is thus not reported here.

Equilibrium constants derived from Gibbs free energies of the reaction further validate the likelihood of the  $\text{DMS} + \text{NO}_3$  reaction in the atmosphere. The  $\Delta G$ ’s of the reaction using MP2, B3LYP, BB1K, MPWB1K, and BH&HLYP are around  $-3$ ,  $-6$ ,  $-10$ ,  $-11$ , and  $-11$  kcal/mol, respectively (see Table 1). The corresponding equilibrium constants, particularly those of the DFT methods, overwhelmingly favor the completion of the reaction. The DFT results should be reliable as the activation energies and the reaction energies are consistent with those of CCSD(T), the highest level of theory in this study.

#### 4. Conclusion

The present study confirms that the  $\text{NO}_3$  radical is a significant contributor to the oxidation of DMS in the troposphere. Because of its strong ability to oxidize at night, ambient nitrate can control the diurnal flux of DMS in areas of high nitrate concentration, as is the case in field studies off the coast of Crete by Bardouki et al. [12] The negative temperature dependence of nitrate can be attributed to negative energy barrier of the reaction as well as the relatively high strength of the reactant complex. Rate constants from BH&HLYP, BB1K, and extrapolated CCSD(T) calculations confirm experimental results while equilibrium constants derived from the  $\Delta G$  values largely favor products over reactants. Future work could be done to understand further oxidation of DMS, including the decomposition pathway of  $\text{CH}_3\text{SCH}_2$  to sulfur dioxide, MSA, and  $\text{CH}_2\text{O}$ . Also, a comparison of the rate of initial DMS oxidation by nitrate to that of OH, Cl,  $\text{O}_3$ , and other radicals would be useful to develop a complete picture of DMS oxidation in the atmosphere.

#### References

- [1] T.S. Bates, B.K. Lamb, A. Guenther, J. Dignon, R.E. Stoiber, J. Atmos. Chem. 14 (1992) 315.
- [2] J.H. Seinfeld, S.N. Pandis, Atmospheric Chemistry and Physics: From Air Pollution to Climate Change, New York, USA, 1998.
- [3] A.M. Winer, R. Atkinson, J.N. Pitts Jr., Science 224 (1984) 156.
- [4] N.R. Jensen, J. Hjorth, C. Lohse, H. Skov, G. Restelli, J. Atmos. Chem. 14 (1992) 95.
- [5] G.S. Tyndall, A.R. Ravishankara, Int. J. Chem. Kinet. 23 (1991) 483.
- [6] N. Gonzales-Garcia, Á. Gonzales-Lafont, J.M. Lluch, J. Comput. Chem. 26 (2005) 569.
- [7] Y. Zhou, D.G. Truhlar, J. Phys. Chem. A 108 (2004) 2715.
- [8] K.B. Wiberg, J.W. Ochterski, J. Comput. Chem. 18 (1998) 108.
- [9] M.J. Frisch et al., GAUSSIAN 03, Revision C.01, Gaussian, Inc., Wallingford, CT, 2004.
- [10] E.P. Daykin, P.H. Wine, Int. J. Chem. Kinet. 22 (1990) 1083.
- [11] S. Zhang, T.N. Truong, Kinetics. CSEO Version 1.0. University of Utah, 2001.
- [12] H. Bardouki, H. Berresheim, M. Vrekoussis, J. Sciare, G. Kouvarakis, L.K. Oikonomou, J. Schneider, N. Mihalopoulos, Atmos. Chem. Phys. Discuss. 3 (2003) 3869.